

Sensor fault diagnosis for nonlinear processes with parametric uncertainties[☆]

Srinivasan Rajaraman^{a,b}, Juergen Hahn^{b,*}, M. Sam Mannan^{a,b}

^a Mary Kay O' Connor Process Safety Center, Department of Chemical Engineering, Texas A&M University, College Station, TX 77843-3122, USA

^b Department of Chemical Engineering, Texas A&M University, College Station, TX 77843-3122, USA

Available online 18 November 2005

Abstract

This paper addresses the problem of detecting, discriminating, and reconstructing sensor faults for nonlinear systems with known model structure but uncertainty in the parameters of the process. The convenience of the proposed technique lies in the fact that historical operational data and/or a priori fault information is not required to achieve accurate fault reconstruction except for fixed, short intervals. The overall fault diagnosis algorithm is composed of a series of nonlinear estimators, which estimates parameter and a fault isolation and identification filter. Parameter estimation and fault reconstruction cannot be performed accurately since faults and parametric uncertainty interact with each other. Therefore, these two tasks are performed at different time scales, where the fault diagnosis takes place at a more frequent rate than the parameter estimation. It is shown that the fault can be reconstructed under some realistic assumptions and the performance of the proposed methodology is evaluated on a simulated chemical process exhibiting nonlinear dynamic behavior.

© 2005 Elsevier B.V. All rights reserved.

Keywords: Fault detection; Fault isolation; Fault reconstruction; State and parameter estimation; Hurwitz stability; Kharitonov's theorem

1. Introduction

There is an impetus to reduce downtime, increase safety, product quality, minimize impact on the environment, and reduce manufacturing costs in modern chemical plants through early and accurate fault detection and diagnosis [1,2]. The need for accurately monitoring the process variables and interpreting their variations increases rapidly with the increase in level of instrumentation in chemical plants. These variations although mostly due to change in operating conditions can also be directly linked to faults. Gathering information about the state of a system and processing the data for detecting, isolating, and identifying abnormal readings are important tasks of a fault diagnosis system [3], where the individual goals are defined as:

- Fault detection: a Boolean decision about the existence of faults in a system.

- Fault isolation: determination of the location of a fault, e.g., which sensor or actuator is not operating within normal limits.
- Fault identification: estimation of the size and type of a fault.

Various techniques exist for performing fault diagnosis [4]. A major portion of these techniques are based upon data from past operations in which statistical methods are used to compare the current operating data to earlier conditions of the process where the state of the process was known. Although these techniques are easier to implement, they have shortcoming that the analysis relies on static models, which assumes that the process operates at a predefined steady-state condition. This is often not the case as the process may undergo throughput changes or exhibit highly nonlinear behavior [5]. Moreover, these methods cannot estimate the shape and size of the fault accurately. Utilizing first-principles-based models into the procedure allows for accurate diagnosis even when operating conditions have changed, while the online estimation of model parameters takes care of plant-model mismatch. The parameter estimation is performed using an augmented nonlinear observer [6,15], which is principally different from often used Extended Kalman filter or Extended Luenberger observer. The proposed fault diagnosis technique itself computes residuals (i.e., the mismatch between

[☆] Seventh Annual Symposium, Mary Kay O'Connor Process Safety Center, Beyond Regulatory Compliance: Making Safety Second Nature, Reed Arena, Texas A&M University, College Station, TX, October 26–27, 2004.

* Corresponding author. Tel.: +1 979 845 3568; fax: +1 979 845 6446.
E-mail address: hahn@tamu.edu (J. Hahn).

the measured output and estimated output using the model) for fault detection [3] and appropriate filters are derived to achieve fault isolation and identification as well. Since it is not possible to simultaneously perform parameter estimation and fault detection, due to the interactions of these two tasks, an approach where these computations are taking place at different time scales is implemented. It is shown that fault detection, isolation, and identification for nonlinear systems containing uncertain parameters can be performed under realistic assumptions with the presented approach.

2. Fault diagnosis for LTI systems

Consider a linear, time-invariant system with no input:

$$\begin{aligned}\dot{x} &= Ax \\ y &= Cx + f_s\end{aligned}\quad (1)$$

where $x \in R^n$ is a vector of state variables and $y \in R^m$ is a vector of output variables, n the number of states, and m refers to the number of output variables. A and C are matrices of appropriate dimensions and f_s is the sensor fault of unknown nature with the same dimensions as the output. Assuming the above system is observable, a Luenberger observer for the system can be designed.

$$\begin{aligned}\dot{\hat{x}} &= A\hat{x} + L(y - \hat{y}) \\ \hat{y} &= C\hat{x}\end{aligned}\quad (2)$$

where L is the observer gain chosen to make the closed loop observer stable and achieve a desired observer dynamics. A residual [3] is defined as:

$$r(t) = \int_0^t Q(t - \tau)(y(\tau) - \hat{y}(\tau)) d\tau \quad (3)$$

which represents the difference between the estimated output and the actual output passed through a filter $Q(t)$. Taking a Laplace transform of Eqs. (1)–(3) results in:

$$r(s) = Q(s)[I - C(sI - (A - LC))^{-1}L]f_s(s) \quad (4)$$

where $Q(t)$ is chosen such that $Q(s)$ is a RH_∞ -matrix [7]. It can be shown that

- (1) $r(t) = 0$ if $f_s(t) = 0$.
- (2) $r(t) \neq 0$ if $f_s(t) \neq 0$.

indicating that the value of $r(t)$ predicts the existence of a fault in the system [7].

In addition, if one uses the dedicated observer scheme as shown for a system with three outputs in Fig. 1, then the fault detection system can also discriminate among various fault sources:

- (3) $r_i(t) = 0$ if $f_{s,i}(t) = 0$, $i = 1, 2, 3, \dots, m$.
- (4) $r_i(t) \neq 0$ if $f_{s,i}(t) \neq 0$, $i = 1, 2, 3, \dots, m$.

where i represents the i th measurement. A fault detection system that satisfies all of the above conditions is called as a fault detec-

tion and isolation filter (FDIF). A fault detection and isolation filter becomes a fault identification filter (FIDF) if additionally the following condition is satisfied [8]:

$$(5) \lim_{t \rightarrow \infty} (r_i(t) - f_{s,i}(t)) = 0, \quad i = 1, 2, 3, \dots, m.$$

In order to meet the above conditions, the following restrictions on the choice of $Q(s)$ are imposed:

- (a) $Q(s) \neq 0$, $\forall s \in C$.
- (b) $Q(s) = [I - C(sI - (A - LC))^{-1}L]^{-1} = C(sI - A)^{-1}L + I$.

Linear, observer-based fault detection, isolation, and identification schemes work well in the event when accurate fundamental model exists for the process over the whole operating region and if appropriate choices are made for L and Q .

3. Robust fault detection, isolation, and identification

3.1. Problem formulation

Consider a nonlinear system with possibly multiple outputs of the following form:

$$\begin{aligned}\dot{x} &= f(x, \theta) \\ y &= h(x, \theta) + f_s\end{aligned}\quad (5)$$

where $x \in R^n$ is a vector of state variables and $y \in R^m$ is a vector of output variables. It is assumed that $f(x, \theta)$ is an infinitely differentiable vector field in R^n and $h(x, \theta)$ is an infinitely differential vector field in R^m . Let $\theta \in R^k$ be a parameter vector assumed to be constant with time but a priori uncertain and f_s is the sensor fault of unknown nature with the same dimensions as the output. The goal of this paper is to estimate the state vector without accurate knowledge of the parameter values describing the process model and under the influence of output disturbances such that $\lim_{t \rightarrow \infty} (x - \hat{x}) = 0$, where \hat{x} is the estimate of the state vector, x and to design a set of filters $Q(t)$ so that the residuals, given by the expression $r(t) = \int_0^t Q(t - \tau)(y(\tau) - \hat{y}(\tau)) d\tau$ have all the five properties discussed in Section 2.

The main challenge in this research is to overcome the effect of sensor faults and plant-model mismatch on the fault identification. In order to perform accurate state and parameter estimation, it is required to have reliable measurements, while at the same time, an accurate model of the process is desired to reconstruct the fault. This will be taken into account by performing the parameter estimation and the fault detection at different time scales. Whenever the parameters are estimated, it is assumed that there is either no fault or fault previously identified remains constant with time, while the values of the parameters are not adjusted during each individual fault detection. A variety of different techniques exist for designing nonlinear closed-loop observers [9–13]. However, since the class of problems under investigation includes parametric uncertainty it would be natural to address these issues through a parametric approach instead of the often used extended Kalman filter or extended Luenberger

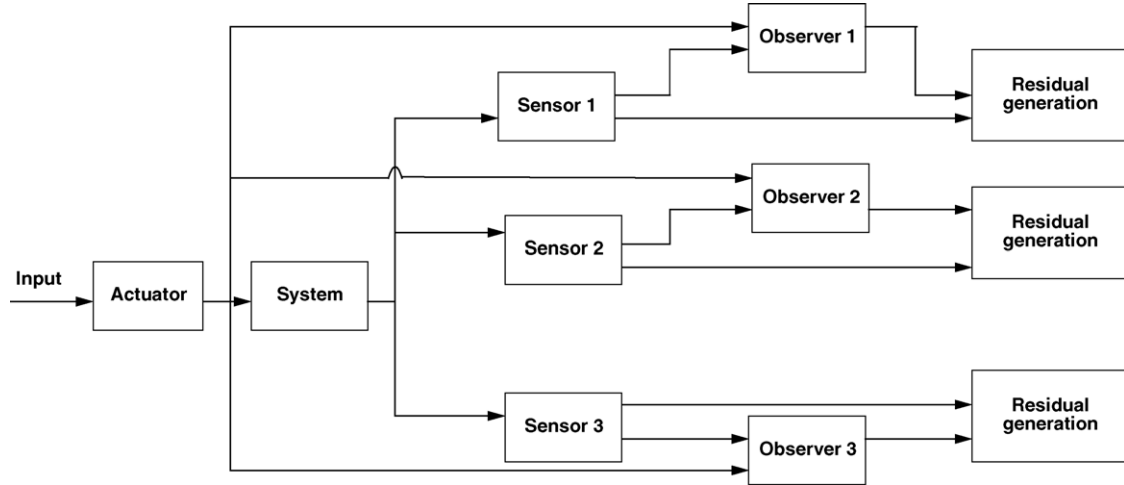


Fig. 1. Schematic of dedicated observer scheme (DOS) for a system with three measurements.

observer. In this paper, authors use an estimator design methodology from their previous work [6,15]. The following subsection briefly discusses parametric approach-based estimator design methodology.

3.2. Observer design methodology

A nonlinear system given by Eq. (5) can be expressed by considering parameters as augmented states of the system:

$$\begin{pmatrix} \dot{x} \\ \dot{\theta} \end{pmatrix} = \begin{pmatrix} f(x, \theta) \\ 0 \end{pmatrix} \quad (6)$$

$$y = h(x, \theta) + f_s$$

and with a change of notation

$$\bar{x} = \begin{pmatrix} x \\ \theta \end{pmatrix}, \quad \bar{f}(\bar{x}, \theta) = \begin{pmatrix} f(x, \theta) \\ 0 \end{pmatrix} \quad (7)$$

this results in the following system

$$\begin{aligned} \dot{\bar{x}} &= \bar{f}(\bar{x}) \\ y &= h(\bar{x}) + f_s \end{aligned} \quad (8)$$

Furthermore, assume that each component θ_i of the parameter vector

$$\theta := [\theta_0, \theta_1, \dots, \theta_{k-1}] \quad (9)$$

can vary independently of the other components and each θ_i lies within an interval where the upper and lower bounds are known

$$\Pi := \{\theta : \theta_i^- \leq \theta_i \leq \theta_i^+, \quad i = 0, 1, 2, \dots, k-1\} \quad (10)$$

Also, let $\theta = \theta_{ss} \in \Pi$ be a vector of constant, a priori unknown parameters and (x_{ss}, θ_{ss}) be an equilibrium point of Eq. (6). The augmented system needs to be observable in order to design an observer, which can also estimate the values of the parameters. The sufficient condition for local observability of the system given by Eq. (6) is discussed with details in an earlier paper [6].

In order to proceed, it is assumed that the augmented system is observable over the entire hyperrectangle-like set Π and the equilibrium points corresponding to these parameters values. It is then possible to design an observer for the augmented system of the following form:

$$\begin{aligned} \begin{pmatrix} \dot{\tilde{x}} \\ \dot{\tilde{\theta}} \end{pmatrix} &= \begin{pmatrix} f(\tilde{x}, \tilde{\theta}) \\ 0 \end{pmatrix} + \bar{L}(\tilde{x}, \tilde{\theta})(y - \hat{y}) \\ \hat{y} &= h(\tilde{x}, \tilde{\theta}) + f_s \end{aligned} \quad (11)$$

where \tilde{x} is the estimate of x , $\tilde{\theta}$ the estimate of θ and $\bar{L}(\tilde{x}, \tilde{\theta})$ is a suitably chosen nonlinear observer gain. The synthesis methodology for the aforementioned nonlinear observer gain is presented in an earlier paper by the current authors [6]. Further, research on enhancing the convergence rates of the above mentioned estimator is presented in [15]. Also, note that the observer makes use of the assumption that the measurement fault is known from an earlier identification of the fault. When the observer is computed for the first time, it has no knowledge about possible sensors faults and assumes that no sensor fault was initially present.

3.3. Fault detection

The fault detection aims to determine whether a fault has occurred in the system. It can be deduced that $\lim_{t \rightarrow \infty} (x - \hat{x}) \neq 0$ in the presence of sensor faults. In order to obtain the information about faults from the system a residual needs to be defined as $r(t) = \int_0^t Q(t - \tau)(y(\tau) - \hat{y}(\tau)) d\tau$, where $Q(t)$ is any stable filter. It can be verified that

- $\lim_{t \rightarrow \infty} r(t) = 0$ if $f_s(t) = 0$.
- $\lim_{t \rightarrow \infty} r(t) \neq 0$ if $f_s(t) \neq 0$.

Additional restrictions on the class of stable filters $Q(t)$ will be imposed in the following sections in order to satisfy desired objectives.

3.4. Fault isolation

Fault isolation is analogous with discriminating among various sources of faults and its computation imposes additional restrictions on the choice of the filter $Q(t)$. In order to perform fault isolation, the augmented system given by Eq. (6) is assumed to be individually observable through each of the outputs $y \forall \theta_{ss} \in \Pi$. This requirement for fault isolation is mandatory for the existence of a fault isolation filter [8], and hence does not pose a stringent condition for using the presented approach.

To achieve fault detection as well as isolation, the proposed approach uses a series of dedicated nonlinear observers as shown in Fig. 1. In this method as many residuals are generated as the number of measurable outputs. It can be verified that

- $\lim_{t \rightarrow \infty} r_i(t) = 0$ if $f_{s,i}(t) = 0$
- $\lim_{t \rightarrow \infty} r_i(t) \neq 0$ if $f_{s,i}(t) \neq 0$ $i = 1, 2, 3, \dots, m$.

for an appropriately chosen filter $Q(t)$.

3.5. Fault identification

In order to estimate the shape and size of the fault, the residuals have to meet the following objective:

$$\lim_{t \rightarrow \infty} (r_i(t) - f_{s,i}(t)) = 0 \quad i = 1, 2, \dots, m$$

Since a dedicated nonlinear observer scheme is utilized in the proposed approach, it remains to choose a suitable stable filter $Q(t)$ to meet all the conditions for fault detection, isolation, and identification. It was shown in Section 2 that an appropriate choice of $Q(t)$ for a linear time, invariant system described by Eq. (1) is given by:

$$Q(s) = C(sI - A)^{-1}L + I$$

where $Q(s)$ is the Laplace transform of the filter $Q(t)$. In this paper, authors use a lower-dimensional observer [6], which does not perform parameter estimation but only estimates the states. A fault identification filter follows from it directly.

In the presence of unknown sensor faults, the estimate of the parameter may diverge from the actual value, and therefore the stability of the overall fault diagnosis system cannot be guaranteed. To overcome this problem, parameter estimation and fault reconstruction are performed at different time scales and it is assumed that the algorithm is initialized when no sensor fault occurs until a time t_0 such that for some $\varepsilon > 0$, $\|y - \hat{y}\|_2 \leq \varepsilon \forall t_0 \geq 0$. The sensor fault is of the following form:

$$f_s(t) = f(t)S(t - t_0), \quad S(t - t_0) = \begin{cases} 1 & t \geq t_0 \\ 0 & t < t_0 \end{cases}$$

The above assumption ensures that the parameter estimate converges to its actual value with a desired accuracy:

$$\|\theta_{ss} - \tilde{\theta}\|_2 \leq \eta, \quad \eta(\varepsilon) > 0 \quad (12)$$

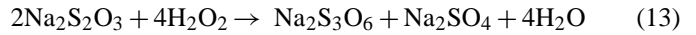
before onset of faults in the original process. Additionally, the parameters are updated periodically by the augmented observer [6] in order to take process drifts into account.

The overall fault diagnosis system performs parameter estimation and fault reconstruction at different time scales, where the fault identification takes place at a higher frequency than parameter estimation. It is assumed that parameter values do not change during the fault identification, while the faults are assumed constant during parameter estimation. Fig. 2 illustrates this two-time scale behavior, where stages 2 and 3 are repeated alternatively throughout the operation and the time between the start of each stage is decided by the nature of the process. However, in general, the parameter estimation is only performed sporadically and requires only short periods of time, so that the fault can be identified for the vast majority of the time.

4. Case study

4.1. Fault diagnosis of a reactor with uncertain parameter

In this section, the main aspects of the proposed fault diagnosis methodology is illustrated through numerical simulations of a nonisothermal CSTR with coolant jacket dynamics, where the following exothermic irreversible reaction between sodium thiosulfate and hydrogen peroxide is taking place [14].



The capital letters A–E are used to denote the chemical compounds $\text{Na}_2\text{S}_2\text{O}_3$, H_2O_2 , $\text{Na}_2\text{S}_3\text{O}_6$, Na_2SO_4 , and H_2O , respectively. The reaction kinetic law is reported in the literature to be [14]:

$$-r_A = k(T)C_A C_B = (k_0 + \Delta k_0) \exp\left(\frac{-E + \Delta E}{RT}\right) C_A C_B$$

where Δk_0 and ΔE represent parametric uncertainties in the model. A mole balance for species A and energy balances for the reactor and the cooling jacket result in the following nonlinear process model:

$$\begin{aligned} \frac{dC_A}{dt} &= \frac{F}{V}(C_{Ain} - C_A) - 2k(T)C_A^2 \\ \frac{dT}{dt} &= \frac{F}{V}(T_{in} - T) + 2\frac{(-\Delta H)_R + \Delta(-\Delta H)_R}{\rho c_p} k(T)C_A^2 \\ &\quad - \frac{UA + \Delta UA}{V\rho c_p}(T - T_j) \\ \frac{dT_j}{dt} &= \frac{F_w}{V_w}(T_{jin} - T_j) + \frac{UA + \Delta UA}{V_w \rho_w c_{pw}}(T - T_j) \end{aligned} \quad (14)$$

where F is the feed flow rate, V the volume of the reactor, C_{Ain} the inlet feed concentration, T_{in} the inlet feed temperature, V_w the volume of the cooling jacket, T_{jin} the inlet coolant temperature, F_w the inlet coolant flow rate, c_p the heat capacity of the reacting mixture, c_{pw} the heat capacity of the coolant, ρ the density of the reacting mixture, U the overall heat transfer coefficient, and A is the area over which the heat is transferred. The process parameters values used for simulations are listed in an earlier paper [6]

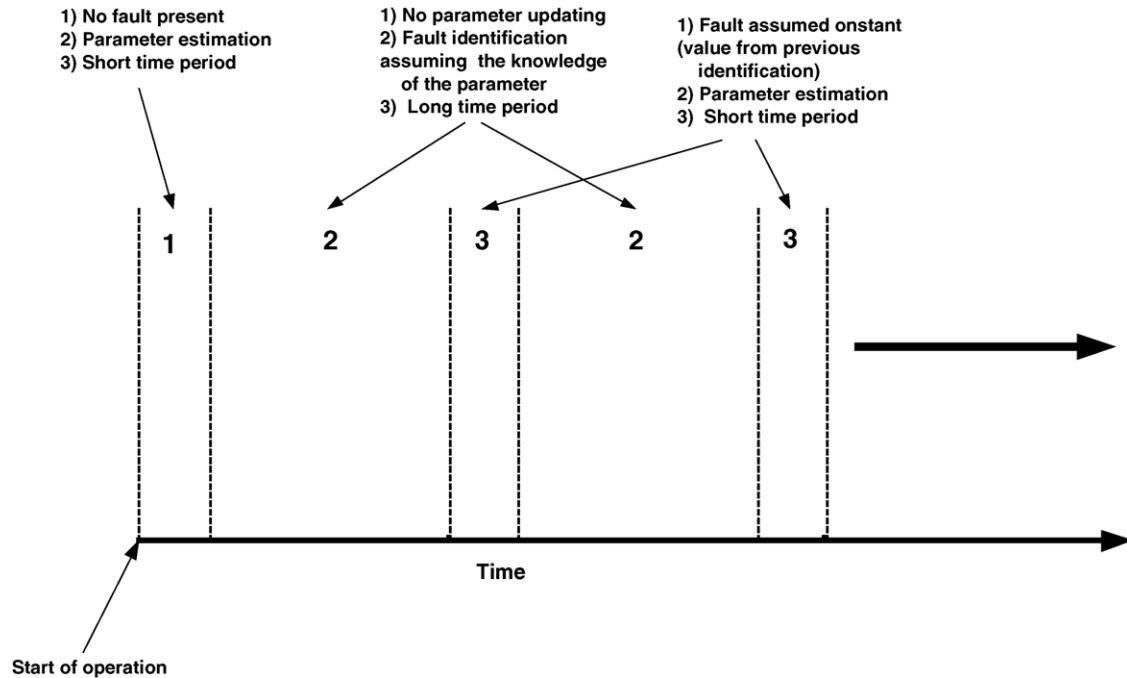


Fig. 2. Schematic fault identification for systems with time-varying parameters.

Here, Δk_o , ΔE , $\Delta(\Delta H)$, and ΔUA represent uncertainty in the pre-exponential factor, the activation energy, the heat of reaction, and the overall heat transfer rate, respectively. When Δk_o , ΔE , $\Delta(\Delta H)$, and ΔUA are all chosen equal to zero, the nominal nonlinear model exhibits multiple steady states, of which the upper steady state (i.e., $C_{Ass} = 0.0192076$ mol/L; $T_{ss} = 384.005$ K; $T_{jss} = 371.272$ K), is stable and chosen as the point of operation. It has been confirmed from simulations that the effect of uncertainty of activation energy on the behavior of the system is higher than the other parameters.

In order to validate the performance of the presented approach, it is in a first step compared to the results derived from a fault detection scheme based upon a Luenberger observer for the process under consideration. For now, the process parameters are assumed to be known. The system matrices obtained by linearizing the process model (14) around the chosen steady state are

$$\begin{bmatrix} \dot{C}_A \\ \dot{T} \\ \dot{T}_j \end{bmatrix} = \begin{bmatrix} -123.74997 & -0.073473 & 0 \\ 17408.48619 & 6.37994 & 2.85714 \\ 0 & 28.57143 & -31.57143 \end{bmatrix} \begin{bmatrix} C_A \\ T \\ T_j \end{bmatrix}$$

$$y_1 = T$$

$$y_2 = T_j$$
(15)

With $\lambda(A) = \{-112.94, -1.37, -34.63\}$. For performing fault isolation and identification, it is required to design observers for each of the two measurements as shown in Fig. 1 and the eigenvalues of the closed loop observers are placed at $\{-6.85, -6.86, -6.87\}$. The observer gain calculated for a measurement

of the reaction temperature is

$$L_1 = \begin{bmatrix} -53.912 \\ 1.55E + 3 \\ 5.79E + 5 \end{bmatrix}$$

and the gain corresponding to the coolant temperature is found to be

$$L_2 = \begin{bmatrix} 1.7E + 2 \\ 2.7E + 4 \\ 1.55E + 3 \end{bmatrix}$$

Both reaction temperature and coolant temperature measurements have zero mean white noise with Gaussian distribution and are induced with an additive sensor fault signal whose shape and size are shown in Fig. 3.

Residuals generated by the technique based upon a Luenberger observer with mismatch in the initial conditions are shown in Fig. 4. Comparing Figs. 3 and 4, it is concluded that the Luenberger observer-based fault diagnosis scheme is able to isolate and identify the approximate nature of the fault in each sensor. Similar simulations have been carried out where the process model includes uncertainties ($\Delta k_o = 5\% k_o$, $\Delta E = 6\% E$, $\Delta(\Delta H) = 5\% \Delta H$, and $\Delta UA = 5\% UA$).

Fig. 5 shows the residual generated for the fault signal shown in Fig. 3 for one specific case of parametric uncertainty. The effect of model uncertainty on the fault diagnosis can be seen from Fig. 5 that while the shape of the fault is reproduced almost perfectly, the bias in the residuals results can be misinterpreted as a response to a step fault in the sensor. To quantify the effect of uncertainty on fault detection, simulations of the fault diagnosis

Table 1
Monte Carlo simulation (with model uncertainty)

Scenarios	Thresholds							
	Luenberger observer with model uncertainty				Presented approach with model uncertainty			
	1	2	3	4	1	2	3	4
00	3.92	9.51	35.80	67.52	100	100	100	100
01	24.01	8.82	44.98	16.80	100	100	100	96.45
10	55.38	55.81	42.20	39.04	89.92	100	100	100
11	76.25	58.18	44.36	16.32	100	100	100	100

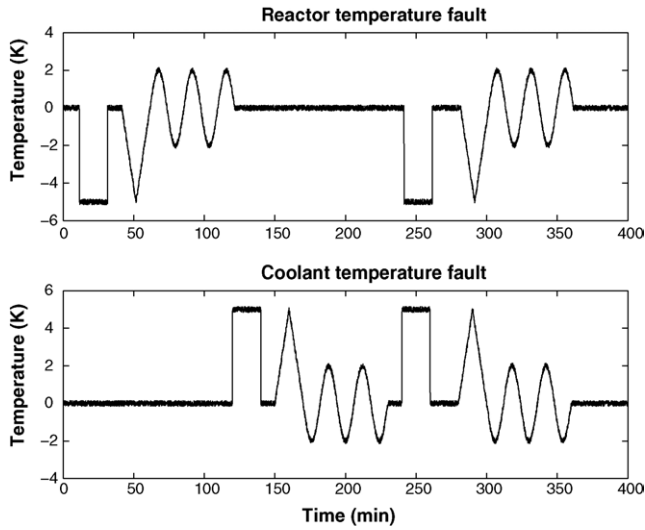


Fig. 3. Reactor and coolant temperature fault signal.

scheme based upon the Luenberger observer are performed for a sufficiently large number of scenarios (10,000) which include a random occurrences of faults in either or both the sensors as well as randomly chosen parametric uncertainty within the given intervals in order to determine the overall percentage of successfully identifying one or all the scenarios. The scenarios

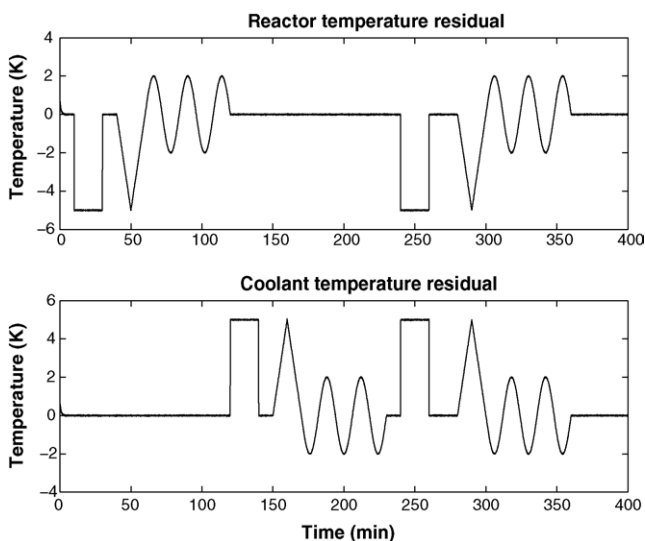


Fig. 4. Reactor and coolant temperature residuals through Luenberger observer scheme (no model uncertainty).

denoted by “00”, “01”, “10”, and “11” in Table 1 stand for no faults in both sensors, no fault in reaction temperature sensor and fault in coolant temperature sensor, fault in reaction temperature sensor and no fault in coolant temperature sensor, and fault in both sensor, respectively. Step faults starting at time $t = 0$ and of magnitude 5 K were added to the sensors. Various thresholds are selected to determine whether or not a fault occurred in either of the sensors and the fault isolation scheme (based upon a Luenberger observer) is tested with Monte Carlo simulations where the parametric uncertainty is chosen at random within the given bounds. To explain this scheme, the scenario identifies the condition where no faults occur in both sensors for a chosen threshold α if the following condition is satisfied:

- if time average of $\frac{1}{T_f} \int_0^{T_f} |r_c(t)| dt < \alpha$, where $r_c(t)$ denotes the coolant temperature residual;
- if time average of $\frac{1}{T_f} \int_0^{T_f} |r_T(t)| dt < \alpha$, where $r_T(t)$ denotes the reactor temperature residual.

where $[0, T_f]$ is the interval over which the time average is calculated.

The criteria used for the other (“01”, “10”, “11”) scenarios are chosen accordingly. Table 1 summarizes the percentage of successfully identifying the correct scenario using the fault isolation scheme in the presence of random uncertainties

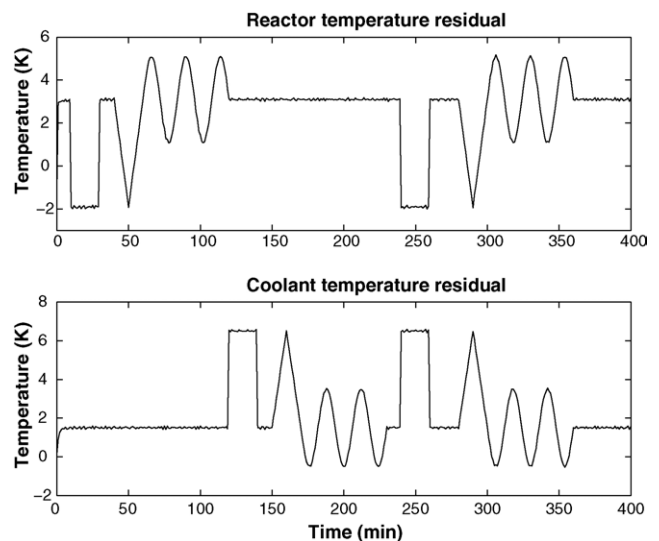


Fig. 5. Reactor and coolant temperature residuals through Luenberger observer scheme (with model uncertainty).

in all the parameters within the range described above. These results show that the parametric uncertainty can have a strong effect on robustness properties of a fault diagnosis scheme, and hence requires techniques that can cope with model uncertainty. The nonlinear fault detection scheme presented in this work is applied to overcome these limitations. Since the effect of uncertainty in the activation energy is greater than the other parameters for fault diagnosis purpose, uncertainty in the activation energy alone $\Pi: = \{E: 0.94E_{ss} \leq E \leq 1.06E_{ss}\}$ is considered $E_{ss} = 76534.704$ J/mol. However, while the design is solely performed based upon uncertainty in this one parameter, the evaluation of the fault diagnosis scheme will consider uncertainty in all of the parameters to compare it to the Luenberger observer scheme.

Using the presented technique and applying it to a system with uncertainty in all of the model parameters, it is found that estimate of the activation energy converges to its true value after 8.4 min in the absence of sensor faults. The assumption that there is no initial sensor fault is a reasonable assumption since one would like to have a certain level of confidence in the measurements before a fault diagnosis procedure is invoked. The coolant and reactor temperature residuals generated by the proposed fault identification techniques for the faults in Fig. 3 are presented in Fig. 5. It is apparent that the residuals converge to the values of the faults even when the uncertainties in the model parameters are a priori unknown. Additionally, the location, shape, and magnitude of the faults are correctly reconstructed and sensor noise is filtered.

Since the performed simulation has only used uncertainty in the activation energy, Monte Carlo simulations have a 100% success rate for the scenarios considered in Table 1. In order to compare the presented fault detection scheme to the Luenberger observer-based one, Monte Carlo simulations are performed taking uncertainty in all the parameters ($\Delta k_o = 5\% k_o$, $\Delta E = 6\% E$, $\Delta(\Delta H) = 5\% \Delta H$, and $\Delta UA = 5\% UA$) into account. The results are summarized in Table 1 and clearly show that the proposed nonlinear fault detection, isolation, and identification scheme performs very well even under the influence of uncertainty in all the model parameters. The assumption that only the activation energy significantly affects the performance of fault diagnosis was a good one, since the fault identification was only designed for uncertainty in this parameter; nevertheless, accurate fault diagnosis is possible even under the influence of uncertainty in all the other parameters. Additionally, it is inferred that it is an important task to choose an appropriate threshold for detecting a fault (Fig. 6).

4.2. Fault diagnosis of a reactor with uncertain and time-varying parameters

Often times processes in chemical industry exhibit a slow change in model parameters with time, e.g., fouling in heat transfer equipment, change in activation energy due to catalyst deactivation, etc. In this section, the performance of the proposed fault diagnosis scheme is evaluated for the nonisothermal CSTR problem as introduced in Section 4.1 but with model parameters varying with time. It has been shown through simu-

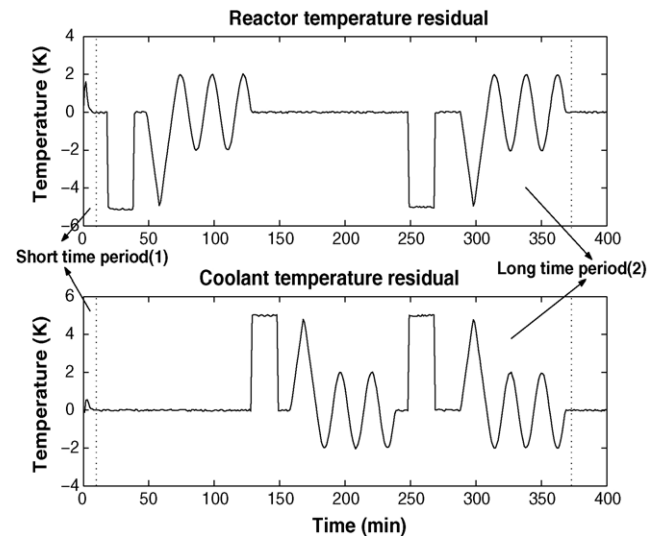


Fig. 6. Reactor and coolant temperature residual signal through presented scheme (with model uncertainty).

lations that activation energy affects the system behavior more than any other parameters, and hence only activation energy is assumed to change with time. Fig. 7 shows the plot of the activation energy and its estimate over the simulated time span and Fig. 8 presents the fault signal $f_s(t)$ that is affecting the sensors. The corresponding coolant and reactor temperature residuals generated by the proposed fault identification technique are shown in Fig. 9. The time period during which the parameter is identified within acceptable limits ranges from $t=0-6$ min. These times were determined by comparing the measured output and the predicted output. The first long time period during which fault detection and identification is invoked ranges from 10 to 415 min. The parameter is adapted from 415 to 422 min. This is followed by another fault detection period ranging from $t=422$ to 782 min. It can be concluded from Fig. 9 that the fault identification scheme is effective even in the presence of time-varying uncertain parameters. It should be noted that the system

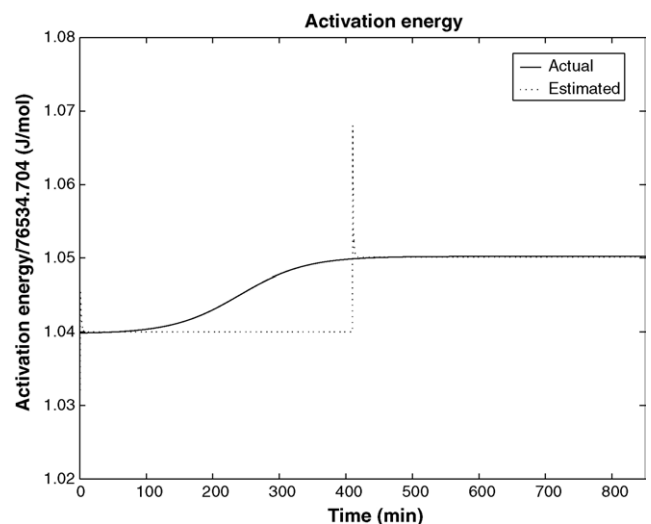


Fig. 7. Activation energy change with time.

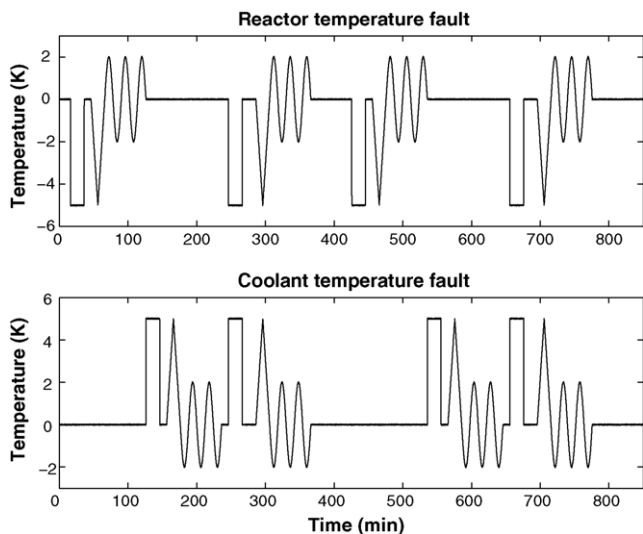


Fig. 8. Reactor and coolant temperature fault signal.

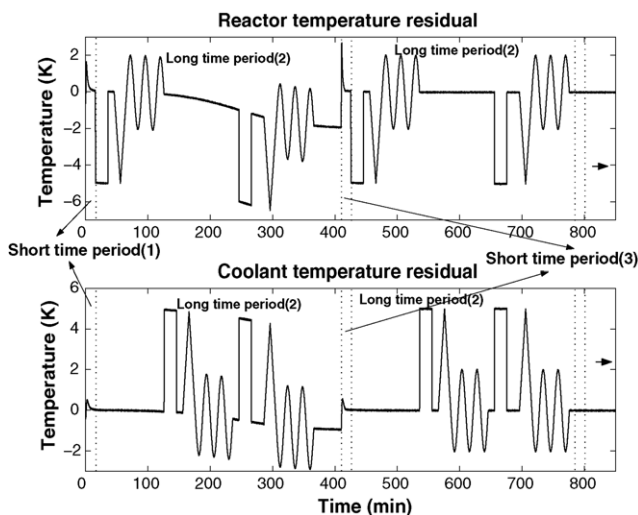


Fig. 9. Reactor and coolant temperature residual signal through presented scheme (with time-varying parametric uncertainty).

would not work as well if the parameters are not periodically re-identified, as can be seen from Fig. 9 during the time period just before 415 min.

5. Conclusions

A new observer-based fault diagnosis scheme for nonlinear dynamic systems with parametric uncertainty was presented. This approach is centered around two main components: the design of an appropriate fault detection, isolation and identification filter for reconstructing the location and nature of the fault and implementation of the aforementioned algorithm with two-time scales. The estimator design for state and parameter estimation was performed based upon authors' prior work [6,15]. The fault isolation and identification filter was designed based upon a linearization of the nonlinear model at each time

step. Repeatedly performing linearization of the model does not pose a problem in practice since it is computationally inexpensive.

Since it is not possible to simultaneously perform parameter estimation and fault detection, these two tasks were implemented at different time scales. The parameters were estimated at periodic intervals where the fault was either assumed to be zero or known and constant, whereas the fault detection scheme was invoked at all times with the exception of the short periods used for parameter estimation.

The performance of the proposed fault diagnosis method was evaluated using a numerical example of an exothermic CSTR and by performing Monte Carlo simulations on a bounded set of parametric uncertainties for a series of faults in both of the available measurements. The faults were reconstructed correctly even in the presence of severe uncertainties in the model parameters and measurement noise.

Acknowledgement

The authors would like to thank Professor Shankar Bhat-tacharyya for his comments in preparation of this manuscript.

References

- [1] F.J. Doyle, Nonlinear inferential control for process applications, *J. Process Control* 8 (1998) 339.
- [2] M. Soroush, State and parameter estimations and their applications in process control, *Comput. Chem. Eng.* 23 (1998) 229.
- [3] J. Chen, R. Patton, *Robust Model Based Fault Diagnosis For Dynamic Systems*, Kluwer Academic Publishers, 1999.
- [4] E.A. Garcia, P.M. Frank, Deterministic nonlinear-observer based approaches to fault diagnosis: a survey, *Control Eng. Pract.* 5 (1997) 663.
- [5] P.M. Frank, X. Ding, Survey of robust residual generation and evaluation methods in observer-based fault detection systems, *J. Process Control* 7 (1997) 403.
- [6] S. Rajaraman, J. Hahn, M.S. Mannan, A methodology for fault detection, isolation, and identification for nonlinear processes with parametric uncertainties, *Ind. Eng. Chem. Res.* 43 (21) (2004) 6774–6786.
- [7] B.A. Francis, *A Course in H_∞ Control Theory*, Springer-Verlag, Berlin, New York, 1987.
- [8] X. Ding, P.M. Frank, Fault detection via factorization approach, *Syst. Control Lett.* 14 (1990) 431.
- [9] D. Bestle, M. Zeitz, Canonical form observer design for nonlinear time-varying system, *Int. J. Control* 47 (6) (1988) 1823.
- [10] S. Othman, J.P. Gauthier, H. Hammouri, A simple observer for nonlinear systems: Applications to bioreactors, *IEEE Trans. Automatic Control* AC-7 (1992) 875.
- [11] G. Bastin, M.R. Gevers, Stable adaptive observers for non-linear time-varying systems, *IEEE Trans. Automatic Control* 7 (1988) 650.
- [12] A.J. Krener, A. Isidori, Linearization by output injection and nonlinear observers, *Syst. Control Lett.* 34 (1998) 241.
- [13] N. Kazantzis, C. Kravaris, Nonlinear observer design using Lyapunov's auxiliary theorem, *Syst. Control Lett.* 34 (1988) 241.
- [14] S.A. Vejtasa, R.A. Schmitz, An experimental study of steady-state multiplicity and stability in an adiabatic stirred reactor, *AIChE J.* 3 (1970) 410.
- [15] S. Rajaraman, J. Hahn, M.S. Mannan, A parametric approach to robust state and parameter estimation for a certain class of nonlinear systems, in: *Proceedings of the 24th American Control Conference*, Portland, OR, 2005.